American Journal of Applied Sciences

Research Article

Multi-Agent Energy Allocation Optimization in Local Energy Communities: A Comparative Study

Amira Dhorbani, Dhaker Abbes, Benoît Robyns and Kahina Hassam Ouari

Department of Electrical Engineering, Univ. Lille, Arts et Metiers Institute of Technology, Centrale Lille, Junia, ULR 2697 L2EP 59000 Lille, France

Article history
Received: 14-03-2025
Revised: 04-07-2025
Accepted: 15-07-2025

Corresponding Author:
Amira Dhorbani
Department of Electrical Engineering, Univ. Lille, Arts et Metiers Institute of Technology, Centrale Lille, Junia, ULR 2697 L2EP 59000 Lille, France
Email: dhorbaniamira7@gmail.com

Abstract: The growing diversity of energy demands, combined with the integration of renewable and distributed energy systems, calls for more adaptive energy management strategies. This study presents a comparative simulation-based analysis of three energy management approaches applied to a local energy community: A Multi-Agent System (MAS), a centralized rule-based method, and a game-theory-based optimization using the Alternating Direction Method of Multipliers (ADMM). The MAS approach models buildings, Electric Vehicles (EVs), and energy storage systems as autonomous agents that dynamically allocate energy based on user preferences. Simulations were conducted using the Multi-Agent Simulation Environment (MESA) framework in Python, with a focus on optimizing energy allocation while minimizing costs and ensuring user comfort. This decentralized approach enables each agent to make local decisions while collectively achieving system-wide objectives. The comparison uses the same use case and dataset across all three methods, ensuring methodological consistency and strengthening the reliability of the performance evaluation. The results demonstrate that the MAS approach achieves lower overall energy costs compared to the rule-based method and ADMM in scenarios prioritizing balanced energy distribution and self-sufficiency, where 'balanced' refers to a scenario that equally weighs user comfort, cost, and local renewable usage objectives. The MAS achieves a total community cost of €359.72 per day in the balanced scenario, compared to €395.54 per day for the rule-based approach and €375.94 per day for the ADMM method, representing cost savings of 9.1 and 4.3%, respectively.

Keywords: Energy Community, Energy Transition, Multi-Agent System (MAS), Optimization, Renewable Energy Sources

Introduction

The global energy transition refers to the ongoing systemic shift in power generation and consumption patterns, driven by the need to reduce dependence on fossil fuels and to integrate low-carbon, renewable energy sources into the grid. This transition is being driven by the need to address climate change, as fossil fuels account for over 75% of the world's greenhouse gas emissions (United Nations, 2024). According to the International Energy Agency (IEA), by 2030, nearly 50% of global electricity is expected to come from solar and wind energy (Sayigh, 2024).

Expanding on this outlook, the IEA's Renewables 2024 report projects a 2.5-fold increase in global renewable electricity capacity by 2030, with a major contribution from rooftop solar and distributed generation systems (International Energy Agency, 2024). This evolution highlights the growing role of decentralized solutions and the active participation of end-users in energy production and management, particularly within energy communities.

This transformation is further accelerated by economic factors. The rapidly decreasing cost of renewable energy technologies, especially solar panels, has made clean energy more accessible. For example, the price of solar panels has dropped by 70% in the past 10 years (Snell and Bazen, 2024), making solar energy a major player in renewable energy integration. However, this rapid

expansion of intermittent renewable sources raises concerns about excess solar and wind power generation and its potential impact on electrical grid stability.

These stability concerns come from the fundamental intermittency of renewable energy sources. These energy sources are not always available; solar energy only works when the sun is shining, and wind energy depends on wind conditions. This variability makes it challenging to use them efficiently within our current energy grids, which were designed for stable energy inputs like coal or gas. To solve this, the concept of energy communities has emerged. These communities consist of local groups or neighborhoods that produce, share, and consume energy together. They can reduce energy costs, improve reliability, and help balance energy use within a community. As energy communities grow and more people become prosumers (those who produce and consume energy at the same time), managing energy distribution becomes more complex. Understanding occupant behavior is crucial for optimizing energy consumption in buildings, as consumption patterns directly influence load forecasting and system efficiency (Yaddarabullah Akbar *et al*., 2023). To handle this, adequate energy management methods must be developed to respond to the needs and to maintain optimal operations. Power system operations have commonly relied on a centralized optimization framework, where all necessary data is gathered, and operational decisions are made centrally by a main controller. But such an approach is encountering significant challenges in emerging power systems. Although centralized control methods may be used to find the best control solutions, they demand significant computational resources to manage the growing volume of data as system size and complexity increase (Olivares *et al*., 2011). In addition, this may lead to a concentration of power in a limited number of entities, potentially creating monopolistic situations (Wen *et al*., 2020; Prehoda *et al*., 2019; Molzahn *et al*., 2017).

In this context, distributed optimization has emerged as an alternative to address the limitations of centralized optimization methods and has gained growing interest.

Qiu *et al*. (2021) investigated scalable coordinated management of Peer-to-Peer (P2P) energy trading using a multi-cluster deep reinforcement learning approach. This work highlights key technical enablers that support the transition from centralized to distributed decision-making in modern energy systems.

Extensive research has been conducted on this topic, Mehdinejad *et al*. (2022) presented a decentralized blockchain-based P2P energy token market for prosumers in a smart grid environment, using a primal-dual sub-gradient method to clear the market. It enables bilateral energy token transactions with a demurrage mechanism to prevent token accumulation and allows consumers to participate in demand response programs. Dong *et al*. (2022) explores strategies to improve trading efficiency while maintaining security and privacy for participants. They propose a game-theoretic approach to dynamically adjust prices based on the market's energy supply and demand.

Game theory is widely used in the energy market to model several interactions, because it offers a powerful framework for analyzing strategic decision-making among multiple stakeholders with conflicting or competing objectives (Tang *et al*., 2019; Bossu *et al*., 2024; Forcan and Forcan, 2023; Stephant *et al*., 2021). Several studies have explored the use of Reinforcement Learning (RL), Deep Reinforcement Learning (DRL), and even multi-agent systems. For instance, a Mixed Deep Reinforcement Learning (MDRL) algorithm was proposed by Huang *et al*. (2022), capable of efficiently managing discrete and continuous hybrid actions in smart home energy management scenarios, effectively minimizing costs while maintaining user comfort. Swibki *et al*. (2023) proposed an energy management approach for a microgrid (MG) based on imitation learning combined with reinforcement learning. Their method, imitation-Q-learning, uses expert demonstrations from linear programming to train the algorithm for decision-making in real-time, reducing energy costs without needing prior knowledge of uncertainties like PV production or electricity prices.

Another promising technique gaining significant attention is the use of Multi-Agent Systems (MAS). Esfahani *et al*. (2019) proposed a multi-agent-based energy management system for multiple grid-connected green buildings. The authors propose using Distributed Energy Resources (DERs) and local energy storage to optimize energy distribution, with each Residential Green Building (RGB) acting as an autonomous agent. Their MAS leverages demand-side management strategies to shift energy use from peak to off-peak hours, enhancing efficiency and profitability. Multiple other studies have also considered using MAS, much of these is directed toward the management and optimization of energy within Microgrids (MG), primarily through strategies involving energy trading (buying and selling) and the use of energy Storage Systems (SS) (Kuruseelan and Vaithilingam, 2019).

While significant progress has been made in the literature, most existing studies focus on specific scenarios, such as isolated microgrids or individual buildings, limiting the generalizability of the solutions. These models may not fully account for the broader context of energy communities, which involve diverse energy actors. Further, many studies focus on optimizing only one or two key performance indicators, such as cost or energy efficiency. However, emerging energy systems require a more pertinent optimization approach that balances multiple objectives.

This study addresses these gaps by proposing a multi-agent-based energy management system designed to handle the complexities of energy communities, which consist of buildings, Electric Vehicles (EVs), and energy storage systems. Our approach stands out by comparing three methods: A centralized rule-based approach, which serves as a calibration benchmark to effectively evaluate the two decentralized methods, one based on the ADMM algorithm and game theory to model the actors, and the other employing a multi-agent system (Stephant *et al*., 2021). All three methods are assessed using the same simulation data to ensure accurate comparisons in balancing multiple objectives, including minimizing energy costs, maximizing renewable energy use, and ensuring user comfort.

In the first section, we introduce various energy management approaches applied to a local university grid, including a rule-based baseline, ADMM approach, and MAS that models user preferences and interactions. The second section presents the results and discusses the comparative performance of each approach, focusing on cost, equity, and self-production metrics across different scenarios. Finally, Section III concludes with insights into the MAS approach's benefits and limitations.

Energy Management Approaches

System Structure

France has taken a leading role in the energy transition by deploying 108 demonstrators across its territory, reinforcing its commitment to sustainability and innovation in energy systems (Gouvy *et al*., 2021). Among these initiatives, the Hauts-de-France region launched the REV3 project in 2013, inspired by the Third Industrial Revolution framework proposed by economist and sociologist Jeremy Rifkin. This initiative seeks to accelerate the shift toward a more sustainable regional economy by integrating renewable energy, digitalization, and circular economic models. Building on the momentum of REV3, the Live Tree project was initiated to transform the Université Catholique de Lille campus in Vauban into an experimental platform for social and technological innovation. Bringing together a network of diverse actors, the project aims to demonstrate novel approaches to energy management while reducing the carbon footprint of the university. At its core, this initiative leverages a smart grid demonstrator that integrates multiple energy technologies, enabling real-world testing of energy optimization strategies.

This demonstrator includes two rooftop photovoltaic systems, with installed capacities of 189 and 28 kWp, respectively, and an Eaton energy storage system (xStorage Building) with a total capacity of 250 kWh. Additionally, it comprises four buildings with distinct energy consumption profiles, six electric vehicle charging stations, and a Point of Common Coupling (PCC) connecting the campus to the local 15 kV power grid via Fronius inverters. The integration of these elements creates an integrated microgrid system that balances local generation, storage, and demand.

Figure 1 provides a graphical representation of the campus infrastructure at Lille Catholic University in the north of France. The microgrid includes four academic buildings HEI1, HEI2, HA, and RIZOMM and is equipped with smart meters and sensors for real-time monitoring and data acquisition. Each physical component is modeled as an autonomous agent in the simulation environment. Buildings act as flexible loads, PV panels are local generation units, EVs are modeled as mobile and time-constrained consumers, and the storage unit serves as a buffer to maintain power balance.

The system integrates two photovoltaic rooftop generators: a 189 kWp PV system (1200 m^2) on the RIZOMM building connected to the grid via ten FRONIUS inverters (ranging from 8.2 to 20 kVA), and a 28 kWp PV system (150 m^2) on the HEI2 building using two 12.5 kVA inverters. A centralized lithium-ion storage system with a total capacity of 250 kWh and a discharge power of 80 kW. Six 22 kW EV charging points are installed and linked through the HA building's LVDB. All components are connected to a 1 MVA, 15 kV/0.4 kV transformer that interfaces the campus with the public distribution grid. The Energy Management System (EMS) communicates with all devices using the Modbus TCP/IP protocol and performs real-time control and forecasting via Python-based scripts. A measurement station monitors all power flows at the main distribution board.

All actors share a single connection point to the external grid, which imposes a global constraint: the total imported power must remain below a predefined subscribed limit. This real-world setup provides a robust platform for evaluating and comparing centralized and decentralized energy management strategies, including rule-based, ADMM, and MAS approaches.

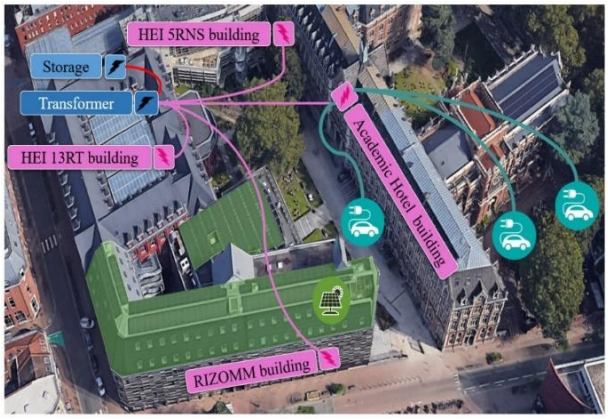

Fig. 1: Lille catholic university demonstrator grid (Swibki *et al*., 2023)

Rule-Based Approach

The first approach tested was a rule-based method used as a benchmark for comparison with other approaches. Starting with a simple example, we assessed its performance to establish a clear baseline, making it easier to compare with more advanced models later.

Utility Functions

Each user *i* has a utility function U_i, representing their satisfaction or well-being by mathematically modeling individual objectives. These functions incorporate personalized preferences through manually set weighting coefficients α, β, γ that are chosen by the users themselves. These coefficients rank the user's priorities, focusing respectively on maximizing cost efficiency, consuming local PV production, and ensuring comfort. The choice of these coefficients is not arbitrary but grounded in established methodologies. In particular, sociological studies conducted in the context of energy communities have identified three core user objectives: minimizing electricity costs, maximizing comfort (i.e., maintaining the desired consumption or production profile), and maximizing the use of locally produced renewable energy (Durillon *et al*., 2020). These objectives form the foundation of the utility functions adopted in our study. To reflect the diversity of user profiles and behaviors, each actor can assign a weight to these three objectives through preference coefficients (α, β, γ), as commonly done in multi-objective optimization frameworks (Marler and Arora, 2010). In order to ensure UsePV Ppvb comparability and consistency across users, these coefficients are constrained to the interval [0, 1] and must sum to 1 for each actor. This normalization guarantees a balanced representation of preferences and allows the optimization process to remain coherent and scalable.

The cost efficiency term is calculated based on the power drawn from the grid, PV-generated power, and battery storage, with their respective costs C_{grid}, C_{pv}, and C_s. The exact methodology used to determine these coefficients, as well as the detailed formulation of the cost efficiency term and the underlying assumptions in its computation, are thoroughly described in Stephant (2021) and Robyns *et al*. (2024). These references provide an in-depth justification for the choice of parameters, the mathematical framework supporting the model, and the empirical validation of the proposed approach.

For example, in a building, the utility function balances these priorities. The user can set a higher α_b if minimizing costs is critical, meaning the system will prioritize drawing from cheaper energy sources. A higher β_b would push the system to use as much PV-generated energy as possible. Finally, a high γ_b would ensure that the building's energy needs are fully met, prioritizing user comfort over cost efficiency.

In the case of EVs, the utility function would prioritize ensuring the battery reaches a desired State of Charge (SOC) by the end of the charging session. A high α_{EV} could reduce charging costs by optimizing when the vehicle charges, while *a* β_{EV} would ensure the EV uses renewable PV energy when available. A high γ_{EV} would focus on fully charging the EV within the available time, ensuring it meets the user's transportation needs. By manually setting these coefficients, each user has the flexibility to tailor their energy usage according to their own priorities, allowing for a personalized and optimized balance between cost, renewable energy usage, and comfort in the energy management system.

Each user has a utility function representing their satisfaction or well-being, balancing cost efficiency, renewable energy use, and comfort. The utility functions for buildings and Electric Vehicles (EVs) are defined as follows.

Buildings: The system includes four buildings, each with varying energy demands that can be met through grid power, PV-generated power, or battery storage. The total demand is defined as P_{totalb}. The proposed utility function for buildings is:

$$\mathrm{U_b} = \alpha_\mathrm{b} \cdot \mathrm{Cost_b} + \beta_\mathrm{b} \cdot \mathrm{UsePV_b} + \gamma_\mathrm{b} \cdot \mathrm{Comfort_b} \quad (1)$$

Where:

$$\mathrm{Cost_b} = \mathrm{C_{grid}P_{gridb}}\Delta\mathrm{t} + \mathrm{C_{pv}P_{pvb}}\Delta\mathrm{t} + \mathrm{C_sP_{sb}}\Delta\mathrm{t} \quad (2)$$

$$\mathrm{UsePV_b} = \frac{P_{pvb}}{P_{totalb}} \quad (3)$$

$$\mathrm{Comfort}_b = \frac{P_b}{\mathrm{P_{bmax}}} \quad (4)$$

Where P_{bmax} represents the maximum power demand of the building, ensuring that the comfort metric is normalized, with a value of 1 indicating that the building's energy needs are fully met and C_{grid}, C_{pv}, and C_s represent the cost per unit of energy from the grid, photovoltaic system, and storage system, respectively, and Δt is the time step used in the simulation.

Parameters:

- α_b, β_b, γ_b: User-defined preferences for cost, *PV* energy use, and comfort
- P_{gridb}, P_{pvb}, P_{sb}: Power drawn by the building from the grid, PV system, and energy storage system, respectively, in each time step Δt
- Electric Vehicles (EVs): For an EV user connected to the charging station, the following utility function is proposed:

$$U_{\mathrm{EV}} = \alpha_{\mathrm{EV}} \cdot \mathrm{CostEV} + \beta_{\mathrm{EV}} \cdot \mathrm{UsePV_{EV}} + \gamma_{\mathrm{EV}} \cdot \mathrm{Comfort_{EV}} \quad (5)$$

Where:

$$\mathrm{CostEV} = C_{\mathrm{grid}} P_{\mathrm{gridEV}} \Delta t + C_{\mathrm{pv}} P_{\mathrm{pvEV}} \Delta t C_s P_{sEV} \Delta \quad (6)$$

DOI: 10.3844/ajassp.2025.20.38

Where C_{grid}, C_{pv}, and C_s represent the cost per unit of energy from the grid, photovoltaic system, and storage system, respectively, and Δt is the time step used in the simulation:

$$UsePV_{EV} = \frac{P_{pvEV}}{P_{totalEV}} \quad (7)$$

Where P_{totalEV} is the total power consumed by the electric vehicle from all sources:

$$ComfortEV = \frac{SOC_{EV}}{SOC_{EVmax}} \quad (8)$$

Where SOC_{EV} is the state of charge of the electric vehicle at arrival time, and SOC_{EVmax} is the maximum state of charge for the EV battery.

Parameters

P_{gridEV}, P_{pvEV}, P_{sEV} : Power drawn by the EV from the grid, PV system, and energy storage system, respectively. For each EV, certain constraints must be considered. According to the current case study, discharging an EV to meet other demands is not allowed, and the charging power is limited by the station's maximum capacity, but only if the EV is connected to the charging station. This is represented by the boolean variable $\delta_{EVi}(t)$, which indicates whether the *EV* is connected at time *t* (1 if connected, 0 otherwise):

$$0 \leq P_{\text{EV}i}(t) \leq P_{\text{EVmax}} \cdot \delta_{\text{EV}i}(t), \quad \forall i \quad (9)$$

In addition, the State OF Charge (SOC) has upper and lower limits, which are characteristics of the vehicle's battery:

$$\text{SOC}_{EVi,\,min} \leq \text{SOC}_{\text{EV}i}(\square) \leq \text{SOC}_{\text{EV}i,\,max} \quad \forall \square \quad (10)$$

For each *EV* connected, we have the state of charge defined as follows:

$$\text{SOC}_{\text{EV}i}(t+1) = \text{SOC}_{\text{EV}i}(t) + \eta_{\text{EV}} \cdot \text{PEV}i(t) \cdot \Delta t \cdot \delta_{\text{EV}i}(t) \quad (11)$$

Where η_{EV} is the efficiency of the electric vehicle under load, and C_{EVi} is the capacity of the vehicle's battery.

Battery storage: We consider the storage system as a full actor within the energy community, meaning it plays an active role in energy exchanges and decision-making. The battery storage unit charges from the grid or PV and discharges to meet the energy needs of buildings and EVs. To optimize its operations, we define a specific utility function for this user, similar to how human users optimize for comfort. In this case, the battery's utility function represents its operational preferences, such as maintaining an optimal SOC, which ensures longevity and efficiency. While the concept of "comfort" traditionally applies to human satisfaction, for the battery, it reflects its need to remain within its preferred operational range to perform optimally:

$$U_s = \alpha_s \cdot \text{Cost}_s + \beta_s \cdot \text{UsePV}_s + \gamma_s \cdot \text{Comfort}_s \quad (12)$$

Where:

$$\text{Cost}s = C_{\text{grid}}.P_{\text{gridCharge}} + C_{\text{pv}} \cdot P_{\text{pvCharge}} + C_s \cdot_{Ps\text{discharge}} \quad (13)$$

Where C_{grid}, C_{pv}, and C_s represent the cost per unit energy from the grid, photovoltaic system, and storage system, respectively:

$$\text{UsePV}s = \frac{\text{P}_{\text{pvCharge}}}{P_{\text{totalCharge}}} \quad (14)$$

Where $P_{totalCharge}$ is the total power used to charge the battery from all sources:

$$\text{Comfort}_s = \frac{\text{SOC}_s}{\text{SOC}_{s\text{max}}} \quad (15)$$

Where SOC_s is the state of charge of the storage system at a given time, and SOC_{smax} is the maximum state of charge for the storage system.

Parameters

$P_{gridCharge}$, $P_{pvCharge}$, $P_{sdischarge}$: Power used to charge the battery from the grid, power used to charge the battery from the PV system, and power discharged from the battery to meet energy needs, respectively. $P_{pvCharge}$, $P_{totalCharge}$: Power drawn from the PV system to charge the battery, and total power used for charging from all sources, respectively. It is important to note that when the battery discharges, it releases energy to meet demand and gain income. This process is represented by a negative value of $P_{sdischarge}$. Moreover, similarly to the EV, the SOC has boundaries:

$$\text{SOC}_{s\,min} \leq \text{SOC}_s \leq \text{SOC}_{s\,max} \quad (16)$$

The power of the battery storage P_s also has operational boundaries, ensuring that it operates within safe and efficient limits:

$$P_{min} \leq P_s \leq P_{max} \quad (17)$$

Similar to electric vehicles, the battery's state of charge is defined by:

$$\mathrm{SOC}_s(t+1) = \mathrm{SOC}_s(t) + \eta_s \cdot \frac{\mathrm{P_s(t)}}{C_b} \cdot \Delta \mathrm{t} \quad (18)$$

Where η_s is the efficiency of the storage system; during charging, $\eta_s = 1$, and during discharging, $\eta_s = 0.98$. We also have C_b that represents its capacity.

Global Constraints

In addition to all these constraints, the integration of multiple energy sources and demands necessitates a careful balance of power within the energy community. The total power generated from the *PV* panels P_{pv}, the power drawn from the grid P_{grid}, and the power from the battery storage unit P_s must collectively meet the energy demands of all users in the system, including the power consumption of the buildings P_{bj} and the electric vehicles P_{EVi}. This requirement is represented by the following power balance equation at each time step *t*:

$$P\mathrm{pv}(t) + P\mathrm{grid}(t) + P_S(t) = \sum P\mathrm{EV}i(t) + \sum P\mathrm{b}\,j\,(t) \quad (19)$$

To further ensure the stability and reliability of the energy system, it is also crucial to limit the power drawn from the grid to within subscribed limits to ensure that the power demand from the grid P_{grid} does not exceed the maximum subscribed power $P_{subscribed\ grid}$:

$$P_{\mathrm{grid}}(t) \leq P_{\mathrm{subscribedgrid}} \quad (20)$$

Methods

In the context of our energy management system, rules are implemented to ensure that energy demands are met while optimizing the use of renewable energy and maintaining system constraints. The decision-making process involves a series of logical checks and conditions that govern power allocation within the system. Depending on these conditions, energy can be sourced from PV panels, the grid, or battery discharge.

A key innovation in our approach is the integration of preference coefficients (α, β, γ) into the decision-making process. These coefficients represent the priorities of different users—buildings, EVs, and storage regarding cost minimization, local PV utilization maximization, and comfort maximization. By incorporating these preferences into the energy allocation strategy, we can tailor power distribution more precisely to meet individual user needs while enhancing overall system performance.

Rule-Based Rules Description

As illustrated in Fig. 2, our energy community consists of multiple types of users. These users provide their preference coefficients, which are utilized in the dynamic allocation algorithm.

The energy dispatch process dynamically allocates available power among different users based on their predefined preference coefficients (α, β, γ), which represent cost minimization, on-site photovoltaic utilization, and comfort priorities, respectively. At each step, the system first assesses the total available energy from photovoltaic (PV) production, battery storage, and the grid.

If PV production exceeds the total demand, it is allocated proportionally to users based on their normalized β coefficients, ensuring that those who prioritize renewable energy receive a higher share. Normalization ensures a fair distribution by summing all β coefficients across users to establish a reference and then dividing each user's β coefficient by this sum to calculate their proportional weight. This normalized weight is then multiplied by the total available PV energy to determine each user's allocated share.

Next, the system transitions to Mode 1, where it checks for any surplus PV energy. If surplus energy is available, it is allocated to charge Electric Vehicles (EVs) based on their normalized β coefficients. If no EVs are connected, the remaining PV energy is stored in the battery. If no surplus PV energy remains for EVs, the system switches to Mode 2.

If PV production is insufficient to cover all the buildings' demand, the system switches to Mode 2, where the remaining energy requirements are met by either discharging the battery or drawing power from the grid, prioritizing the lowest-cost option based on real-time grid and storage prices. The allocation of grid and storage power follows a similar proportional distribution, using users' α and γ coefficients to prioritize those seeking cost minimization while maintaining system constraints such as maximum subscribed grid power and state-of-charge limits.

This preference-based allocation ensures that energy distribution is both fair and efficient, aligning with individual user priorities while optimizing overall system performance.

ADMM Approach

This approach, (Stephant *et al*., 2021) differs from the previous centralized rule-based method by adopting a distributed framework. In this model, each participant optimizes its energy profile independently according to individual goals, such as minimizing costs, enhancing comfort, or maximizing local energy exchanges, using customized weighting in a utility function. The (ADMM) Alternating Direction Method of Multipliers) algorithm is employed to improve this decentralized control, allowing users to optimize locally while ensuring coordination at the community level.

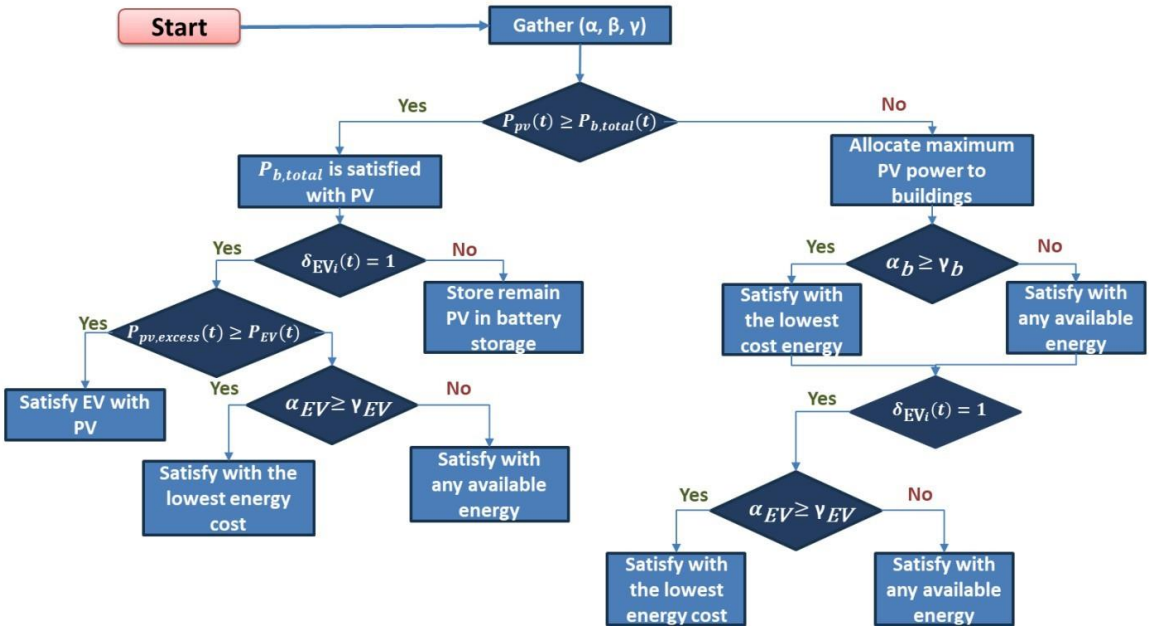

Fig. 2: Rule-based system design

The algorithm can be explained as follows: let $\bar{x}$ denote the average of all x_i, *i.e.*:

$$\bar{x} = \frac{I}{N} \sum_{i=1}^{N} x_i$$

Two new variables, z and u, are introduced, defined on the same domain as $\bar{x}$. We define the primal and dual residuals at iteration $k + 1$ as:

$$r^{k+1} = x^{k+1} - z^{k+1}, s^{k+1} = \rho(z^{k+1} -> z^{k})$$

The algorithm terminates when both residuals are smaller than their respective thresholds $\varepsilon^{\text{primal}}$ and $\varepsilon^{\text{dual}}$, ensuring that z is sufficiently close to $\bar{x}$ and stable across iterations. The algorithm is written as follows (with $\|.\|$ denoting the Euclidean norm):

Algorithm 1: ADMM Algorithm
1: **while** $r^k > \varepsilon^{\text{primal}}$ and $s^k > \varepsilon^{\text{dual}}$ **do**
2: $x_i^k \leftarrow \text{argmin}_{xi} (-U_i(x_i) + \frac{\rho}{2} \| - x_i^k x^{-k} - Z^k u^k \|^2)$
3: $z^{k+1} \leftarrow \text{argmin}_z (g(Nz) + \frac{N\rho}{2} \| z - u^k - x^{-k+1} \|^2)$
4: $u^{k+1} \leftarrow u^k + x^{-k+1} - z^{k+1}$
5: **end while**
6: return $X = [x_1, \ldots, x_N]$

In the first step (line 2), each agent locally optimizes its utility function Ux according to its own preferences and constraints. The term $\frac{\rho}{2} \| x_i - x_i^k + x^{-k} - z^k + u^k \|^2$ is a penalty term applied equally to all agents to enforce compliance with global constraints. Lines 3 and 4 correspond to an aggregation step: All local solutions xi are collected, then the variable z is updated by considering the global constraints represented by the function g. The dual variable u is also updated. At the end of each iteration, the penalty term $L^k = \bar{x}^k - z^k + u^k$ is transmitted to all agents for the next iteration. The parameter ρ is the penalty weight. In practice, a larger value of ρ encourages faster convergence toward satisfying global constraints, at the cost of possibly reducing the agents' individual utilities. The choice of this parameter has a significant impact on the final results. Some studies suggest adjusting ρ adaptively at each iteration to balance convergence speed and solution quality.

In the context of our case study, the abstract mathematical variables of the ADMM algorithm map directly to the physical actors and decision variables within the energy community, as shown in Fig. 3. Each variable x_i corresponds to the local decision vector of agent i, which includes its power allocation from PV, battery storage, and the grid at each time step. For instance, for a building, x_i captures the quantities of power it decides to consume from each available source based on its preferences (α, β, γ) and current demand. Similarly, for an EV, x_i includes the charging power schedule, while for the storage unit, it includes charging or discharging decisions. The global variable z represents the aggregated consensus profile that ensures the overall energy balance and compliance with shared constraints, such as the total grid import not exceeding the subscribed limit. In our system, this includes ensuring that the sum of all agents' demands remains within the available generation and subscribed power

thresholds. The dual variable u can be interpreted as a feedback signal that each agent receives from the system to align its local decision x_i with the global coordination variable *z*. For example, if too many agents simultaneously draw power from the grid, the corresponding u will penalize this behavior in the next iteration, pushing agents to adjust their strategy (e.g., favor PV or battery usage). Finally, the penalty parameter ρ governs how strongly the agents are pushed to follow the collective agreement *z*. A high ρ enforces tighter adherence to global constraints, such as the grid import limit, but may reduce the ability of agents to optimize their individual utility functions. Therefore, choosing ρ appropriately is essential for achieving a balance between local autonomy and system-wide coordination.

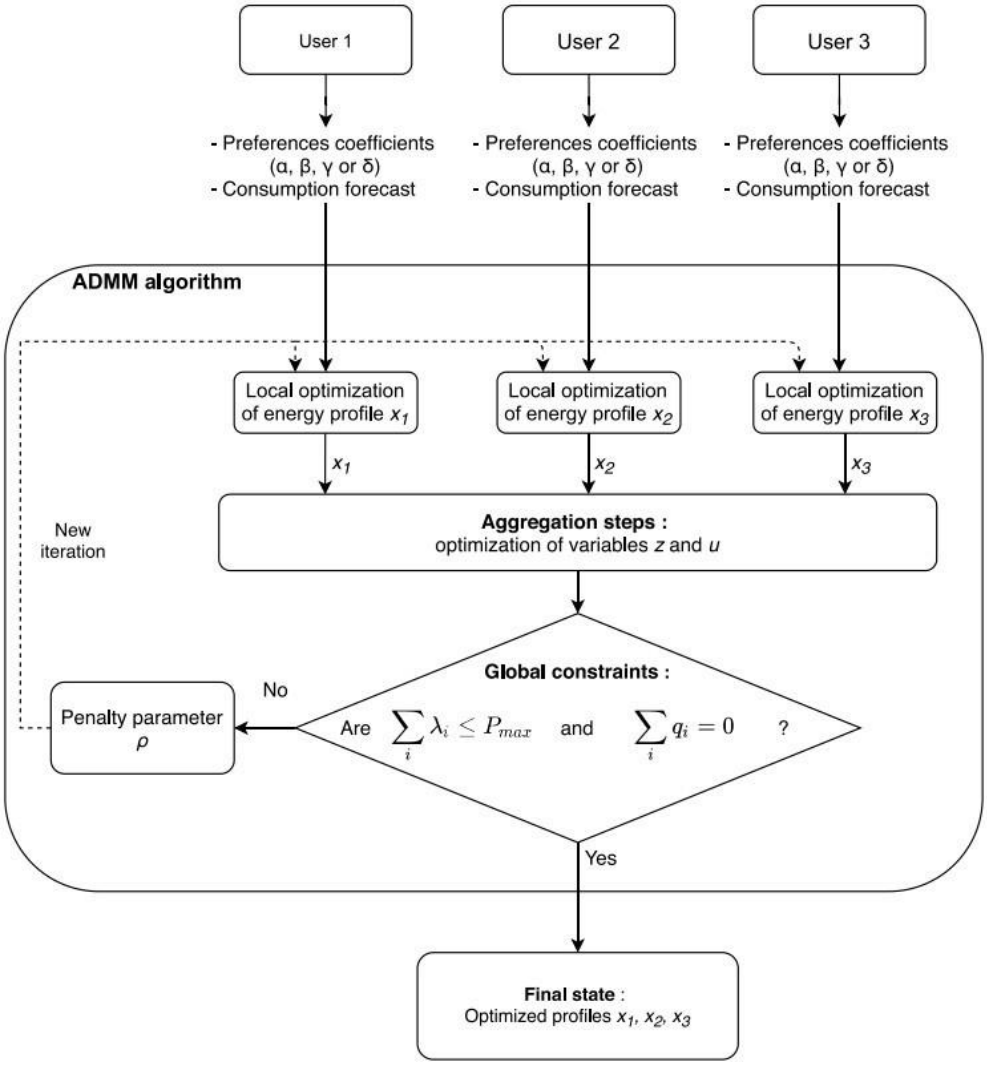

Fig. 3: Optimization overview using ADMM (Stephant *et al*., 2021)

Multi-Agent Approach

Definition

According to the definition of MAS Poole and Mackworth (2010) an agent is comprised by a coupling of perception, reasoning and acting components. Perception allows the agent to gather information from its environment through sensors, providing a representation of the state of the external world. Reasoning enables the agent to process the perceived information, make decisions, and develop plans or strategies to achieve its objectives. The reasoning component often involves the application of logical inference, decision-making algorithms, or machine learning techniques. Finally, the acting component allows the agent to perform actions in its environment via actuators, influencing the external world and potentially interacting with other agents. In a multi-agent system, these individual agents can interact either cooperatively or competitively, leading to complex, emergent behaviors that result from their local

interactions. The system's overall performance depends on how well the agents can coordinate, communicate, and adapt to achieve shared or individual objectives (Dorri *et al*., 2018). Figure 4 shows the Perception-Action-Goal-Environment (PAGE) model of an agent in a multi-agent system. This model highlights the cyclical interaction between the agent and its environment. The agents in a multi-agent system can be classified into three categories: passive agents, active agents, and cognitive agents. Each category differs based on the complexity of its behavior, the level of autonomy, and the capacity for decision-making and reasoning. A passive agent, often referred to as a reactive agent, is an agent without a specific target or purpose, characterized by limited communication capabilities and the ability to respond only to commanded actions from other agents or external inputs. These agents do not initiate actions on their own but react to stimuli in their environment. On the other hand, an active agent operates with defined goals, meaning it can act independently to achieve specific objectives, guided by pre-set rules or strategies. The most advanced type, the cognitive agent, is capable of handling complex computations, reasoning, and mutual communication with other agents. Cognitive agents are designed to learn from their interactions, adapt to changing environments, and collaborate with other agents to achieve more sophisticated tasks. The choice of MAS in this study is driven by the complexity and diversity of energy consumption behaviors within energy communities. We saw that it would be particularly interesting to model users as individual agents within the system. This approach allows for more accurate modeling of user preferences, energy allocation behaviors, and interactions with renewable energy sources. In addition, increased adaptability and scalability are other reasons. As energy systems evolve and expand, MAS can easily scale by adding more agents to represent new users or devices, without the need for centralized reconfiguration.

System Description

To describe the MAS, it is necessary to define the PAGE where the agents act. The PAGE of the proposed multi-agent system is presented in Table 1. In this multi-agent energy management system, each agent has a utility function similar to the centralized approach and operates within an environment with varying energy demand profiles, PV generation, storage capacity, and grid constraints. The percepts for the agents include data such as current energy demand, available PV power, storage SOC, and grid capacity. Based on these percepts, the agents perform actions like allocating energy from PV, storage, or grid to meet their demand, charging or discharging storage, and managing grid power consumption. The goals of the agents differ depending on their preferences, whether to minimize energy costs, maximize comfort by meeting energy demands, or maximize PV usage. The environment they operate in consists of the fluctuating energy demand, variable PV output, storage limits, and the costs associated with different energy sources, all of which influence the agents' decisions and interactions within the system. Each agent's actions contribute to the overall system's efficiency and cost-effectiveness, reflecting a cooperative system.

At the core of the agent are its state, which captures its current condition or data, and its rules, which guide how the agent responds to various situations. These internal components work together to determine the agent's actions, which are the decisions or outputs generated in response to the agent's understanding of its state and the applied rules. The agent then executes these actions, which directly influence the environment, while also being influenced by the inputs and conditions provided by the environment. Interactions among agents are implemented through direct method calls within each agent's step () function. Agents iteratively negotiate energy allocation by exchanging state and preference information, computing utilities, and dynamically adjusting energy requests. Conflicts arising when multiple agents simultaneously request limited resources (e.g., PV or battery power) are resolved using a priority-based method that is clearly implemented.

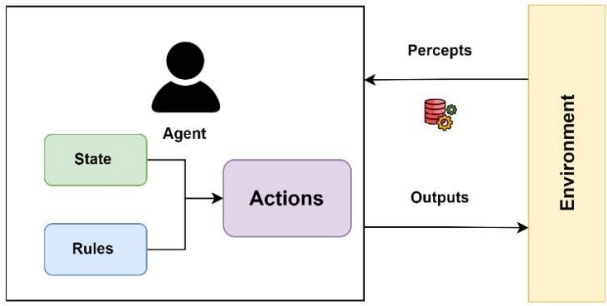

Fig. 4: PAGE Model Diagram

Table 1: Agent characteristics in the energy management system

Agents	Description
Percepts	$P_b(t), P_{pv}(t), P_s(t), P_{grid}(t)$, C_{grid}, C_{pv}, C_s, $SOC_{EV}(t)$, $SOC_{EV_{max,\,min}}$, δ_{EV} $SOC_s(t)$, $SOC_{s\ max,\,min}$, $P_{subscribed_{grid}}$
Actions	: Allocate power from PV, storage, or grid; charge EV using PV, storage, or grid; discharge/charge battery storage
Goals	: Depending on preferences α,β,γ: minimize cost, maximize PV usage, maintain a high level of comfort
Environment	: Shared environment of interactions

Power Allocation Within Users

The multi-agent system described is defined by a collection of autonomous agents making independent decisions based on local conditions and interacting directly with each other to balance energy supply and demand. At the core of this system is a specific class, which functions as the central hub for resource allocation and state management. This class is responsible for initializing and managing all agents, ensuring they operate in a coordinated and efficient manner. It only serves as a framework to organize and coordinate the simulation, managing the timing of the agents' actions and collecting data across the system. The actual decision-making and energy allocation processes such as determining how much energy a building or EV will draw from PV, storage, or the grid, are handled by the agents themselves within their respective "step" methods defined in each agent class. The agents decide based on their own needs, preferences, and the availability of energy resources, and they interact with each other. Communication between agents is implemented through direct message passing, where each agent queries others about their energy availability, state-of-charge, and preference coefficients at each timestep. Negotiations between agents occur iteratively based on the comparison of calculated utility values derived from their preference coefficients. When multiple agents simultaneously request more resources than are available (such as PV or battery storage energy), conflicts are resolved using a priority-based strategy. High-priority requests those emphasizing comfort are addressed first, followed by renewable-energy-focused requests, and lastly those focused on cost minimization

For example, the building agent begins by checking its energy demand for the current time step and then queries the PV agent to determine the available PV energy. It calculates the portion of its demand that can be met by PV, constrained by its preference for PV energy. After consuming this energy, the building reduces its demand accordingly and updates the PV agent on the energy used. If the demand remains unmet, the building checks the storage agent's available energy, considering both the storage capacity and its preference for storage energy, or uses energy from the grid to fully meet its demand if the costs are low. The agent continuously adjusts its consumption to ensure the total energy used matches its demand, and it calculates the total cost based on the energy consumed from each source.

Results and Discussion

For our multi-agent system developed with Python, we used the same data employed in the previous two methods to allow a direct comparison. As seen in Fig. 5, the cost of grid power Cg varies between 0.05 and 0.15 C/kWh. The cost of photovoltaic power Cpv is fixed at 0.1 C/kWh. The cost of discharging stored energy Cs varies between 0.35 and 0.4 C/kW.

The optimization simulation is conducted for a full day, 10-06-2019, starting at midnight (00:00) and ending 24 hours later (24:00). The cost information used in this study is fixed according to Stephant *et al*. (2021), ensuring consistency for comparison.

The production data shown in Fig. 6 is the same used across all methods to ensure consistency in the comparison. It should be noted that while the comparative analysis presented in this study assumes perfect knowledge of energy generation, demand, and pricing for fair comparison purposes, the practical implications of forecast uncertainties have been thoroughly investigated in a separate analysis. This complementary study, conducted over 7 days using real versus predicted data, demonstrated that the proposed MAS maintains robust performance even under realistic forecast errors. Specifically, the system exhibited only a 1.4% increase in total community costs when operating with forecasted data compared to actual measurements, while preserving identical comfort levels and maintaining the same high PV self-consumption efficiency. However, in this study, we deliberately choose to work with the assumption that predicted values equal real values to ensure consistency and enable direct comparison with the other methods using the same dataset from (Stephant *et al*., 2021).

Physical Parameters of Different Users

This section presents the physical parameters used to model the different actors. In total, there are 4 EVs, 2 PVs, one battery, and 4 buildings. The characteristics of the 4 EVs and the battery are summarized in Tables 2 and 3 below. It may be noted that the battery's state of charge is relatively low, but this configuration is maintained to keep the data consistent with previous studies, allowing for effective comparisons afterward.

Table 2: Physical parameters of electric vehicles

Characteristics EV1		EV2	EV3	EV4
tarrival	9:15	10:30	11:00	10:00
tdeparture	12:30	19:00	16:30	18:00
SOCEVimin	20%	45%	40%	25%
SOCEVimax	100%	100%	100%	100%
SOCEVirequired	60%	80%	80%	85%
PEV_{max} (kWh)	22	22	7.2	22
ηVE	80%	80%	80%	80%

Table 3: Physical parameters of battery storage

Characteristics	Battery
SOC_{min}	10%
SOC_{max}	100%
$SOC_{required}$	35%
P max charge (kW)	40
Pmaxdischarg (kW)	80
Ecapacity (kW) 40	203

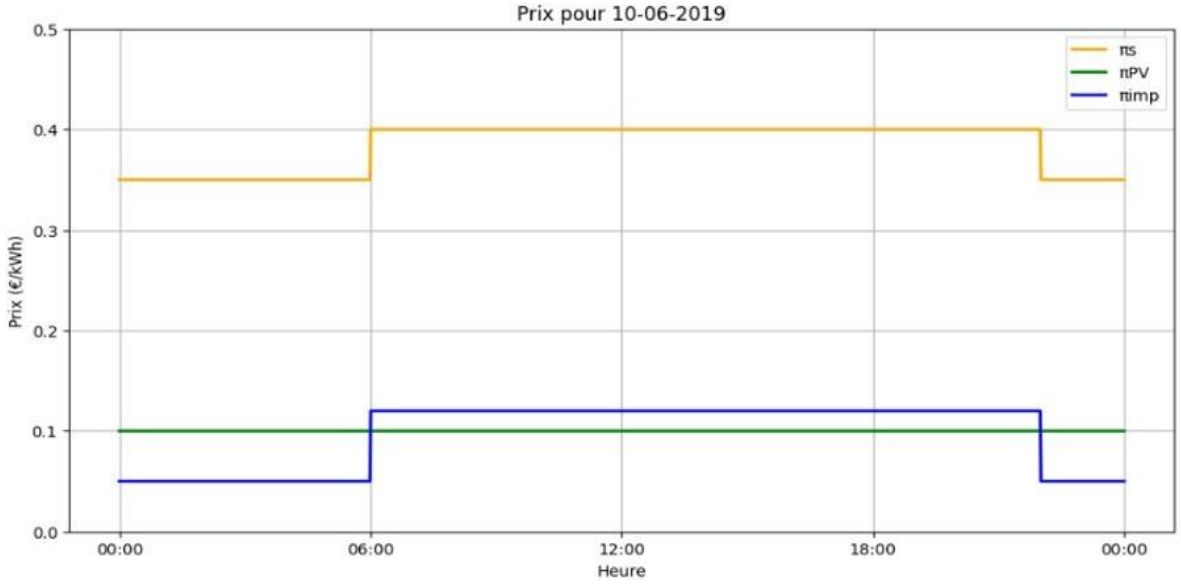

Fig. 5: Energy prices

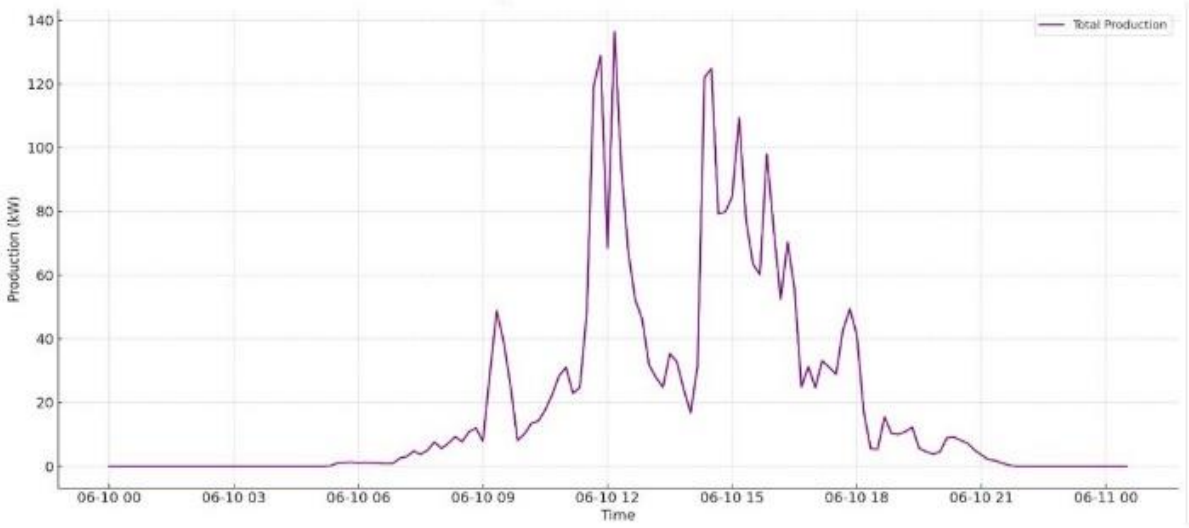

Fig. 6: PV production

Scenarios and Results

Several scenarios were tested in this case to evaluate the robustness of our algorithm. The same scenarios as in Stephant *et al*. (2021) were applied here. These scenarios capture a range of actor behaviors, and we distinguish five specific cases:

- An economic scenario where actors aim to reduce their costs or maximize their profits (denoted as I). Practically, agents prefer cheaper energy sources, potentially sacrificing comfort or renewable utilization
- A scenario where users prioritize their comfort (denoted as II). Agents ensure full energy demand satisfaction, often leading to higher dependency on grid energy despite higher costs
- A scenario in which actors primarily focus on exchanging energy within the community (denoted even as III). This maximizes local self-consumption and reduces reliance on external energy sources
- A balanced scenario that incorporates elements of the first three (denoted as IV). This scenario closely mirrors realistic energy community objectives by balancing cost efficiency, renewable usage, and user comfort
- A scenario where random coefficients are assigned to each user (denoted as V). This reflects realistic community diversity, with unpredictable and varied user priorities

The scenarios are determined according to preference coefficients, as shown in Table 4.

Table 4: Preferences (α, β, γ)

User	Scenario I	Scenario II	Scenario III	Scenario IV	Scenario V
VE1	0.8,0.1,0.1	0.1,0.1,0.8	0.1,0.8,0.1	0.33,0.33,0.33	0.31,0.29,0.40
VE2	0.8,0.1,0.1	0.1,0.1,0.8	0.1,0.8,0.1	0.33,0.33,0.33	0.43,0.08,0.49
VE3	0.8,0.1,0.1	0.1,0.1,0.8	0.1,0.8,0.1	0.33,0.33,0.33	0.10,0.80,0.10
VE4	0.8,0.1,0.1	0.1,0.1,0.8	0.1,0.8,0.1	0.33,0.33,0.33	0.10,0.80,0.10
Battery	0.8,0.2,-	0.5,0.5,-	0.2,0.8,-	0.5,0.5,-	0.2,0.8,-
PV	0.8,0.1,0.1	0.1,0.1,0.8	0.1,0.8,0.1	0.33,0.33,0.33	0.10,0.80,0.10
Building 1	0.8,0.1,0.1	0.1,0.1,0.8	0.1,0.8,0.1	0.33,0.33,0.33	0.10,0.80,0.10
Building 2	0.8,0.1,0.1	0.1,0.1,0.8	0.1,0.8,0.1	0.33,0.33,0.33	0.10,0.80,0.10
Building 3	0.8,0.1,0.1	0.1,0.1,0.8	0.1,0.8,0.1	0.33,0.33,0.33	0.10,0.80,0.10
Building 4	0.8,0.1,0.1	0.1,0.1,0.8	0.1,0.8,0.1	0.33,0.33,0.33	0.10,0.80,0.10

When comparing these results to the centralized rule-based approach (Table 5), the rule-based method incurs higher costs, particularly in Scenario III, where it reaches -460 €.

When comparing these results to the distributed method used in Stephant *et al*. (2021), the total community cost is consistently higher in Stephant *et al*. (2021) using ADMM, especially in Scenario III, where the cost is -381.40 €, compared to -363.86 € in our study. Similarly, in the balanced Scenario IV, ADMM results in a cost of -375.94 €, which is significantly higher than the -359.72€ in this study. Even in Scenario I, where both studies prioritize cost minimization, the total cost is slightly higher in study Stephant *et al*. (2021) (-369.46 €) compared to our study (-371.96 €).

Overall, our method demonstrates lower community costs across most scenarios, particularly in Scenario III (energy exchange) and Scenario IV (balanced strategy), while Stephant *et al*. (2021) using the ADMM algorithm tends to result in slightly higher total costs for the community.

Performance Indicators

Global Constraints

As shown in Fig. 7, the total grid consumption for the MAS method consistently remains below the imposed grid limit of 580 kW on a winter day. Likewise, during a summer day, the grid consumption also stays within this limit, as illustrated in Fig. 8. These results confirm that the MAS method operates efficiently across different seasons. More specifically, Fig. 7 shows that during the winter day, grid power usage peaks between 7:00 and 17:00 across all scenarios due to limited solar generation, with the system approaching but not exceeding the grid limit. Figure 8 highlights a different trend: the summer profile benefits from higher PV availability around midday, resulting in reduced grid dependency and lower peak values. These patterns demonstrate the MAS's ability to adapt to seasonal production differences while ensuring that grid constraints are never violated, regardless of user preferences. To verify the robustness of the proposed system, simulations were conducted for both winter and summer days, ensuring that the MAS performs reliably under varying environmental and production conditions.

Equity and Self-Production

Equity indicator: We calculate the equity indicator, which quantifies the distribution of a shared resource among N actors (in our case, photovoltaic energy). Equity ranges from 0 to 100, with 100% indicating a perfectly equitable distribution of the resource among all actors. A value close to 0% suggests a concentration of the resource among a small number of actors, reflecting a highly unequal distribution. The indicator represents the quantity of the resource allocated to actor *i*.

As seen in Table 6, the multi-agent system achieves an average equity of 35%, which is better than the 22% seen with the rule-based algorithm but lower than the 55% achieved by the ADMM algorithm. This shows that the multi-agent system is fairer than simple rule-based methods, but doesn't perform as well as the ADMM approach in distributing resources evenly. One reason for this could be that in a multi-agent system, each agent tends to optimize its own outcome, rather than the overall equity of the system. To improve our system, we will focus on enhancing communication and coordination between agents. We will also explore implementing additional mechanisms that encourage agents to prioritize equity by introducing constraints or reward systems that promote more balanced decision-making across the agents.

Table 5: Comparison of Total Costs Paid (€) per day

	ADMM Stephant *et al*. 2021)	Rule-based approach	MAS
I	-369.46	-430.3	-371.96
II	-382.47	-390.23	-390.93
III	-381.4	-460.06	-363.86
IV	-375.94	-395.54	-359.72
V	-366	-388.76	-365.89

Table 6: Equity indicator for different methods

Method	MAS	Rule-Based	ADMM
Equity (%)	35	22	55

DOI: 10.3844/ajassp.2025.20.38

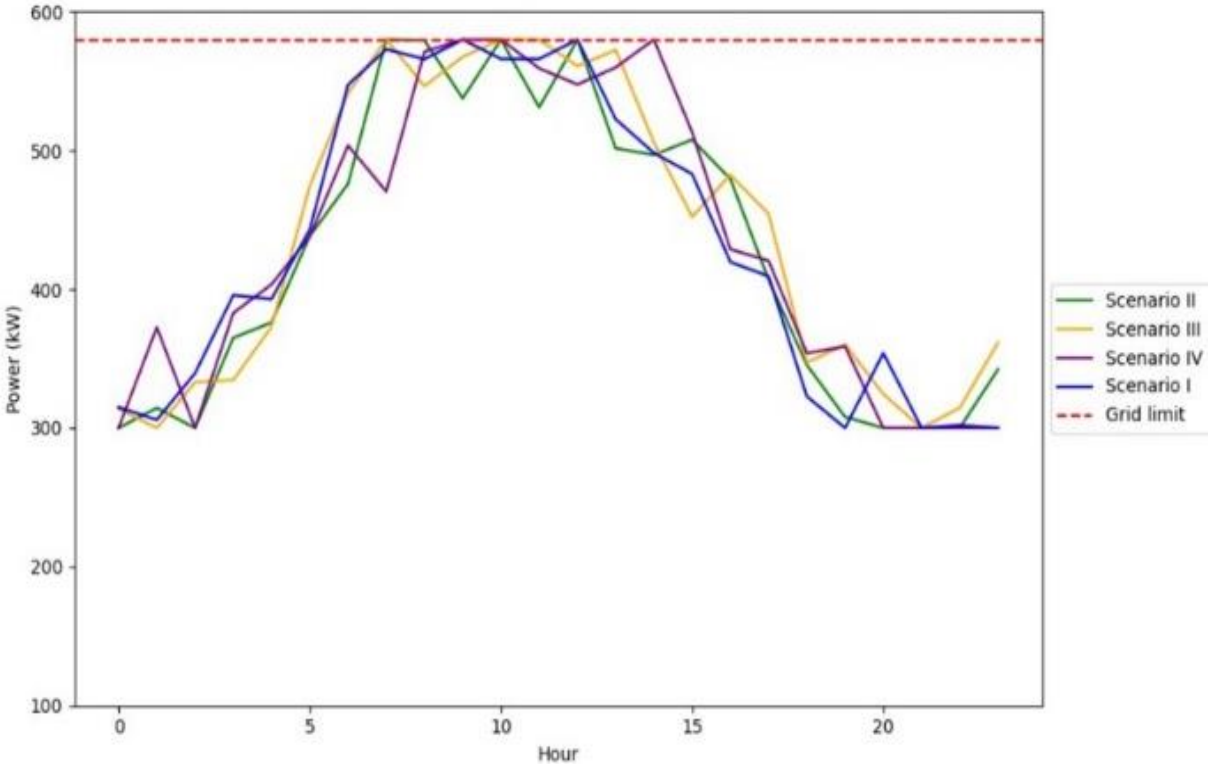

Fig. 7: Imported Grid power on a winter day

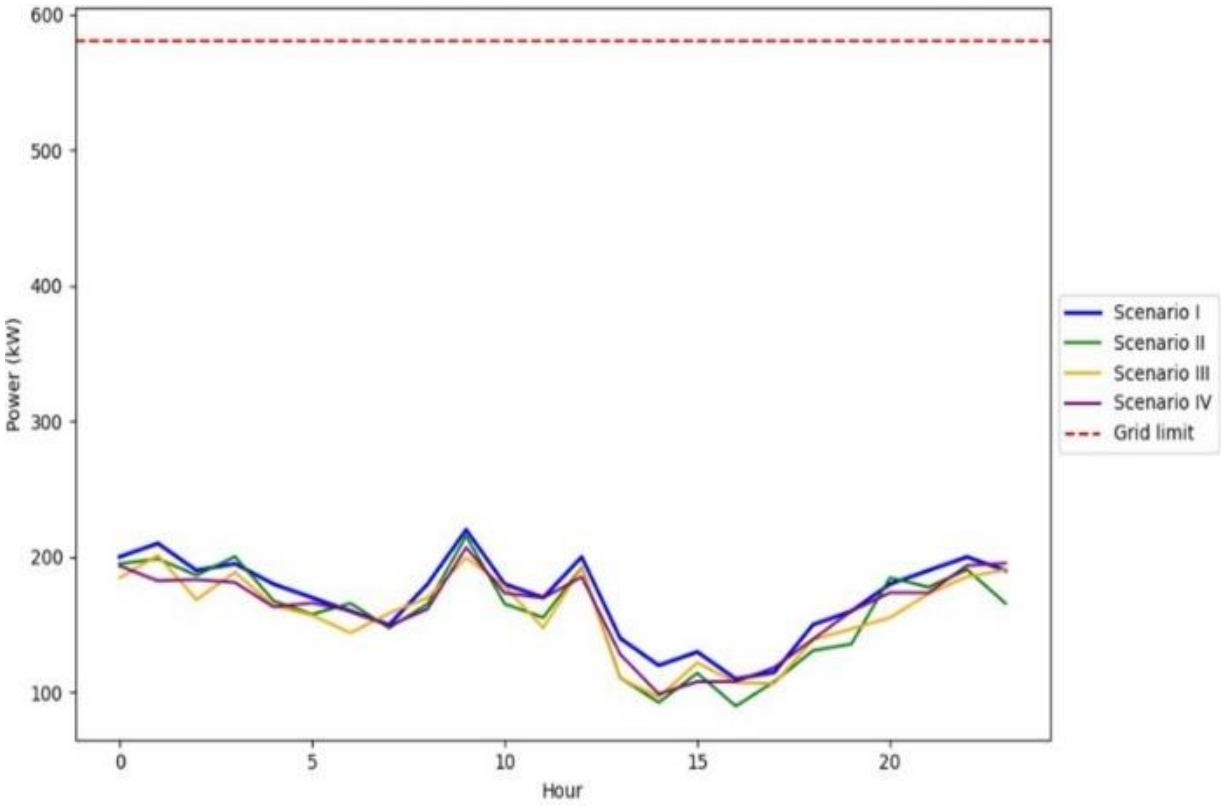

Fig. 8: Imported Grid power on a summer day

Self-production we also calculated the self-production rate represented in Table 7, which quantifies the amount of consumed energy that comes from locally produced sources. This rate provides insight into how much of the energy demand is met by PV production rather than relying on other energy sources. A higher self-production rate indicates greater energy independence and efficiency, as more of the energy consumed is being produced locally, reducing the need for energy imports and enhancing sustainability.

When comparing the self-production rates of the multi-agent system and ADMM across different scenarios, the multi-agent system shows higher performance in Scenario III (focused on energy exchange) and Scenario V (random coefficients), with self-production rates of 15 and 18.71%, respectively, compared to ADMM's consistent rate of around 11.5% (Stephant *et al*., 2021). However, in Scenarios I and II, which prioritize cost reduction and user comfort, respectively, ADMM performs better. This suggests that the multi-agent system is more effective in increasing energy self-sufficiency when there is a focus on energy exchange or when the system is flexible.

In the next subsection, we will delve further into the multi-agent system approach, especially Scenario IV, the balanced scenario, because it represents an equilibrium between minimizing costs, exchanging energy within the community, and maintaining user comfort. Scenario IV stands out as it offers the lowest total community cost (-359.72€), demonstrating its effectiveness in balancing multiple objectives compared to other strategies. We will further develop our analysis by examining the power allocation profiles among users, specifically focusing on how energy is distributed between them. By analyzing these power profiles and the key performance indicators, we can better understand the mechanisms behind the reduced community costs.

Results Based on Scenario IV for Multi-Agent Approach

Power Profiles and State of Charges

Figure 9 shows the power profile for buildings over a 24-hour period, with the load consistently fluctuating between approximately 15 and 100 kW. The PV contribution is visible primarily during daylight hours, peaking around midday, suggesting that solar energy is being used when it is available, reducing the load on other energy sources.

Table 7: Self-production rate (MAS)

	I	II	III	IV	V
Self-production rate	7.92 %	8.10 %	8.10 %	13.81 %	18.71 %

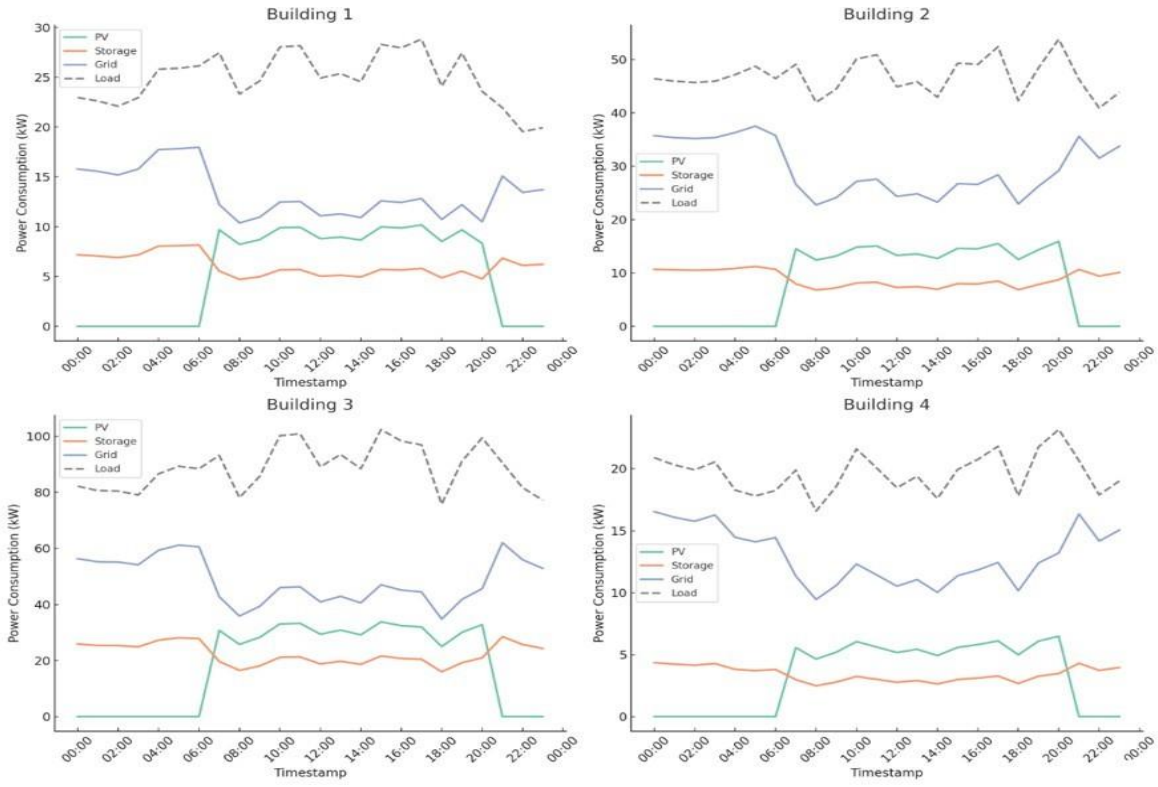

Fig. 9: Power profiles for buildings

The energy distribution across the buildings is quite balanced and follows a similar pattern, reflecting that the equal preference coefficients (α, β, γ) have been respected consistently across the buildings. In all buildings, the grid is the dominant energy source, ranging from about 44.5 to 57% as seen in the pie charts (Fig. 10). This observation aligns with the grid import profile depicted in Fig. 8, which corresponds to the summer day used for the Scenario IV simulation. The reliance on the grid is primarily because PV energy is only available during daylight hours, and storage capacity is not always sufficient to fully meet the buildings' energy demand. Thus, the grid acts as a fallback to ensure that energy needs are met consistently, especially during periods of low solar production or high demand.

We also present SOC of each EV (Fig. 11), the graph shows the charging behavior of four EVs, each with different arrival and departure times. All vehicles start charging upon arrival and reach 100% state of charge before their respective departures. This ensures that user comfort is fully met, as all EVs are fully charged when needed.

Agent Activity Indicators

Figures 12 and 13 display the total number of interactions for each agent in the multi-agent system, reflecting the roles and actions of these agents in the energy management strategy and the total number of interactions. The PV, Storage, and Grid agents show the highest levels of interaction, indicating their central role in the system as they work to manage and distribute energy among the other agents. These agents frequently interact with other components due to their significant responsibilities in allocating energy resources, as evidenced by their high interaction counts. All the buildings have the same number of interactions, which is because they request energy at each time step, consistently engaging with the other agents (PV, Storage, and Grid) to meet their energy demands. EVs, on the other hand, have fewer interactions because they only engage with the system when they are connected to the charging station, specifically between their arrival and departure times. The notably high interaction count for the storage agent is explicitly due to its frequent decision-making behavior. At every time step, the storage agent proactively interacts with other agents, repeatedly evaluating opportunities to charge or discharge energy depending on instantaneous system conditions. This high interaction frequency is thus event-driven, originating from continuous evaluations triggered at every simulation step rather than mere polling or random interactions.

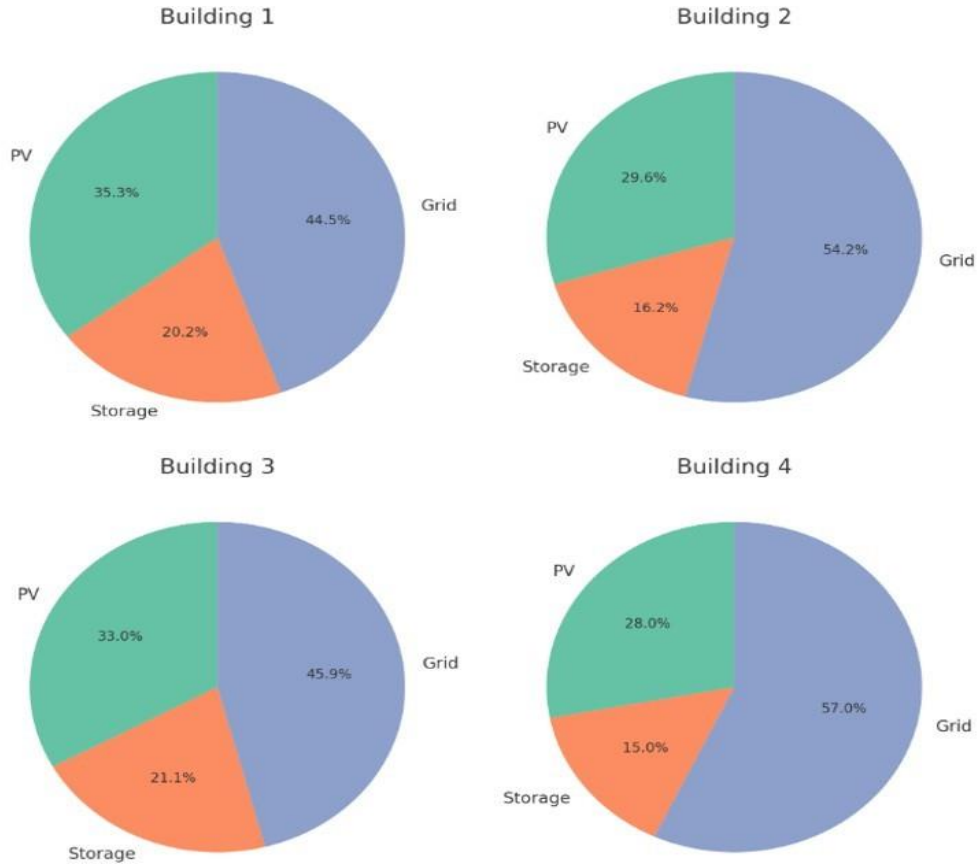

Fig. 10: Power source distribution

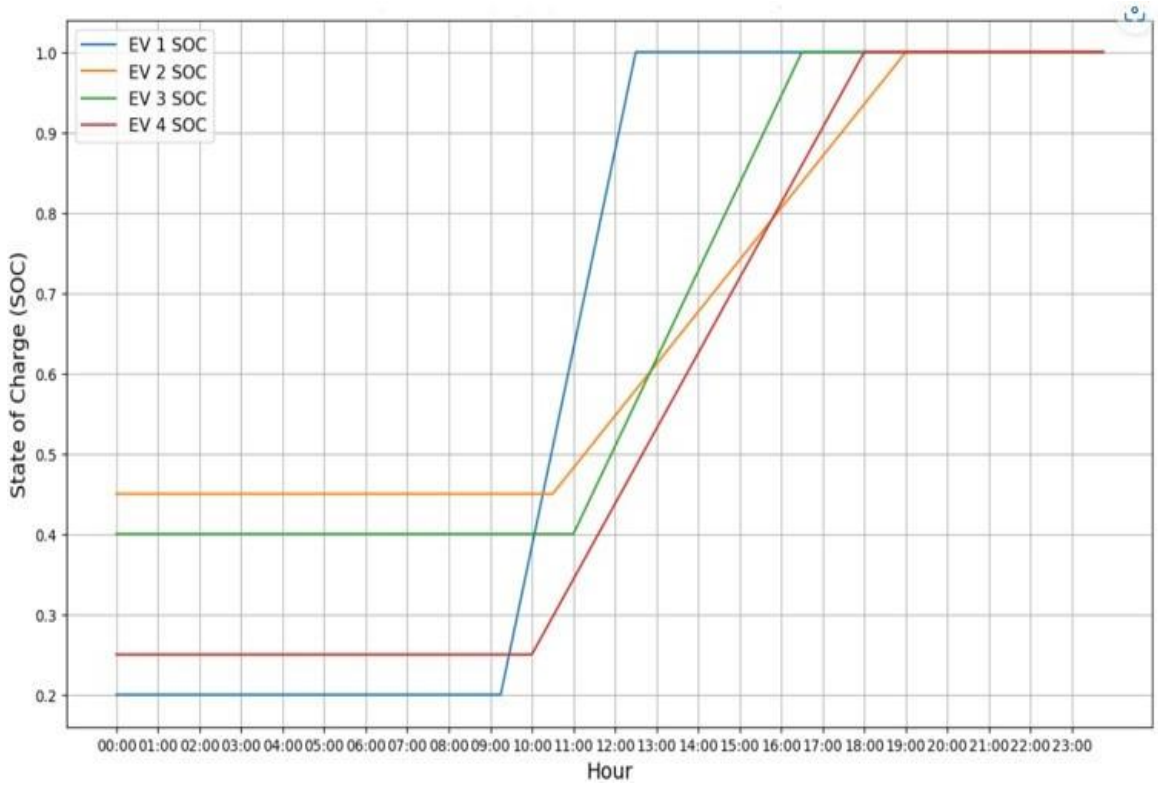

Fig. 11: EVs State of Charge

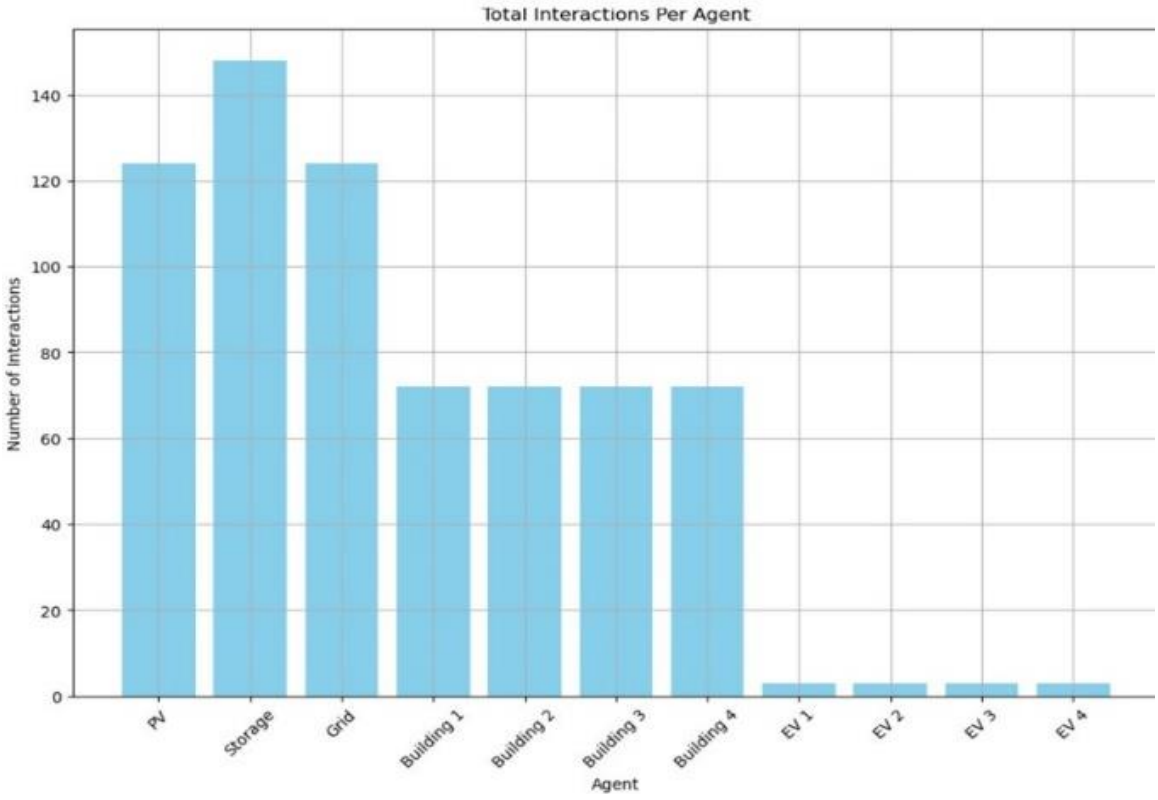

Fig. 12: Total interactions per Agent

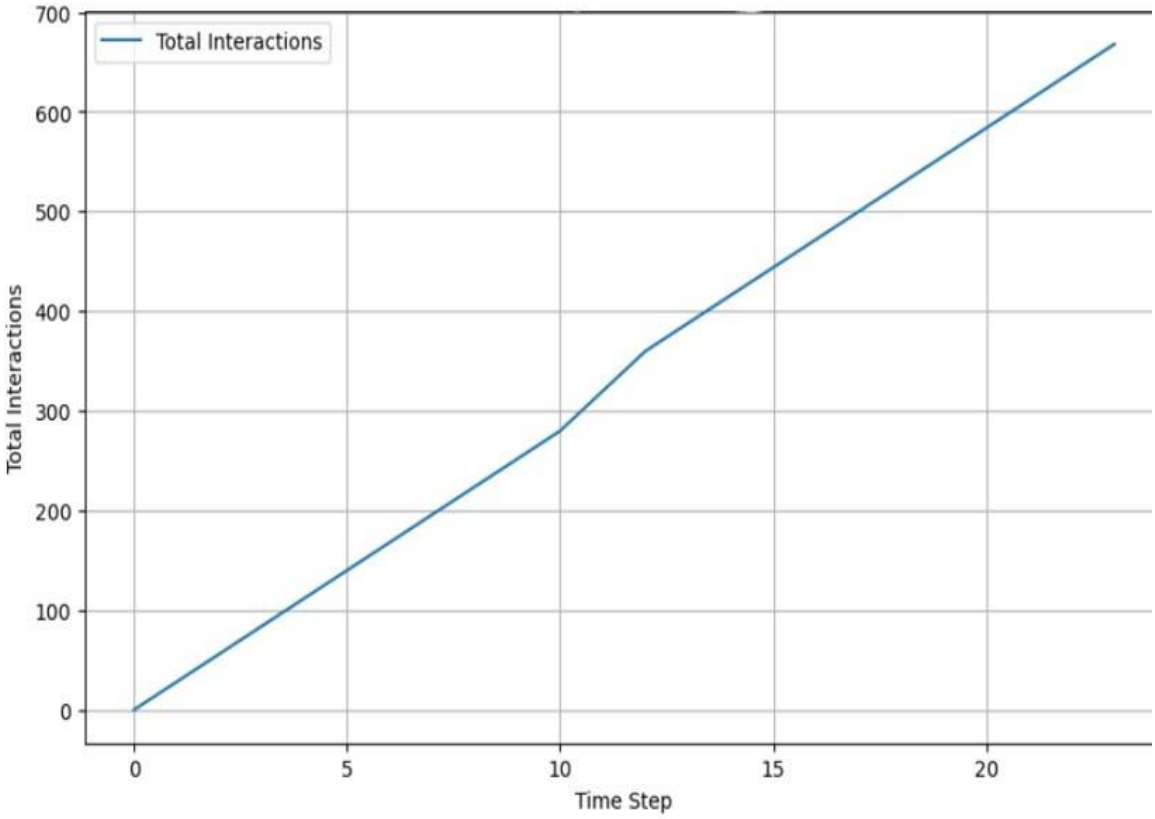

Fig. 13: Total interactions evolution

Conclusion

In this study, we demonstrate the potential of multi-agent systems for energy management within energy communities compared to two other methods. By leveraging autonomous agents representing different types of users, the MAS was able to dynamically allocate energy resources, optimize costs, and maintain user comfort, achieving lower total community costs compared to other approaches. However, the approach has its limitations. First, the equity distribution of energy among agents is still suboptimal compared to ADMM-based solutions, indicating that the MAS prioritizes local optimization over system-wide fairness. Second, the interaction frequency, especially for agents like storage, can lead to unnecessary computational overhead, as agents continuously check for conditions that might not result in action. Future work will focus on overcoming these limitations by improving agent coordination and communication. One area of development is enhancing the equity of energy distribution by introducing constraints or reward mechanisms that encourage agents to consider the overall system's fairness. Also, testing the MAS in larger-scale, real-world environments will be essential to validate its scalability and adaptability in more complex energy systems.

Acknowledgment

This work has been supported by the French National Research Agency (ANR) under the program AI Engineering PhD@Lille. It was also conducted within the framework of the EE4.0 (Energie Electrique 4.0) project. EE4.0 is co-financed by the European Union through the European Regional Development Fund (ERDF), with the financial support of the French State and the Hauts-de-France Region.

The authors would also like to thank the Catholic University of Lille for providing access to the smart grid demonstrator data and for enabling the use case studied in this research.

Authors Contributions

Amira Dhorbani: Conceptualization, methodology, software, validation, formal analysis, investigation, data curation, writing original draft, and visualization.

Dhaker Abbes and Benoît Robyns: Supervision, methodology, and writing review and edited.

Kahina Hassam Ouari: Supervision, methodology, validation, and writing review and edited.

Ethics

The data used in this work were collected from the Lille Catholic University smart grid demonstrator with

the agreement of the institution. No personal or sensitive information was used in this study. All methods were carried out in accordance with relevant guidelines and regulations. The authors declare that there are no ethical issues associated with the research presented in this paper.

References

Bossu, A., Durillon, B., Davigny, A., Barry, H., Robyns, B., Belaïd, F., & Saudemont, C. (2024). Coalitional game-based gain generation and distribution for collective self-consumption in an energy community. *Mathematics and Computers in Simulation*, *225*, 129–147. https://doi.org/10.1016/j.matcom.2024.04.012

Dong, J., Song, C., Liu, S., Yin, H., Zheng, H., & Li, Y. (2022). Decentralized peer-to-peer energy trading strategy in energy blockchain environment: A game-theoretic approach. *Applied Energy*, *325*, 119852. https://doi.org/10.1016/j.apenergy.2022.119852

Dorri, A., Kanhere, S. S., & Jurdak, R. (2018). Multi-Agent Systems: A Survey. *IEEE Access*, *6*, 28573–28593. https://doi.org/10.1109/access.2018.2831228

Durillon, B., Davigny, A., Kazmierczak, S., Barry, H., Saudemont, C., & Robyns, B. (2020). Decentralized neighbourhood energy management considering residential profiles and welfare for grid load smoothing. *Sustainable Cities and Society*, *63*, 102464. https://doi.org/10.1016/j.scs.2020.102464

Esfahani, M. M., Hariri, A., & Mohammed, O. A. (2019). A Multiagent-Based Game-Theoretic and Optimization Approach for Market Operation of Multimicrogrid Systems. *IEEE Transactions on Industrial Informatics*, *15*(1), 280–292. https://doi.org/10.1109/tii.2018.2808183

Forcan, J., & Forcan, M. (2023). Behavior of prosumers in Smart Grid: A comparison of Net Energy Metering and Billing Schemes, and Game Theory-based Local Electricity Market. *Sustainable Energy, Grids and Networks*, *34*, 101058. https://doi.org/10.1016/j.segan.2023.101058

Gouvy, N., Nassar, J., & Lefévère, V. (2021). Transforming the Catholic University of Lille Campus into a Smart Grid. *Organizing Smart Buildings and Cities*, *36*, 177–184. https://doi.org/10.1007/978-3-030-60607-7_11

Huang, C., Zhang, H., Wang, L., Luo, X., & Song, Y. (2022). Mixed Deep Reinforcement Learning Considering Discrete-continuous Hybrid Action Space for Smart Home Energy Management. *Journal of Modern Power Systems and Clean Energy*, *10*(3), 743–754. https://doi.org/10.35833/mpce.2021.000394

International Energy Agency. (2024). *Renewables 2024: Analysis and forecast to 2029*.

Kuruseelan, S., & Vaithilingam, C. (2019). Peer-to-Peer Energy Trading of a Community Connected with an AC and DC Microgrid. *Energies*, *12*(19), 3709-. https://doi.org/10.3390/en12193709

Marler, R. T., & Arora, J. S. (2010). The weighted sum method for multi-objective optimization: new insights. *Structural and Multidisciplinary Optimization*, *41*(6), 853–862. https://doi.org/10.1007/s00158-009-0460-7

Mehdinejad, M., Shayanfar, H., & Mohammadi-Ivatloo, B. (2022). Decentralized blockchain-based peer-to-peer energy-backed token trading for active prosumers. *Energy*, *244*, 122713. https://doi.org/10.1016/j.energy.2021.122713

Molzahn, D. K., Dorfler, F., Sandberg, H., Low, S. H., Chakrabarti, S., Baldick, R., & Lavaei, J. (2017). A Survey of Distributed Optimization and Control Algorithms for Electric Power Systems. *IEEE Transactions on Smart Grid*, *8*(6), 2941–2962. https://doi.org/10.1109/tsg.2017.2720471

Olivares, D. E., Canizares, C. A., & Kazerani, M. (2011). A centralized optimal energy management system for microgrids. *2011 IEEE Power and Energy Society General Meeting*, 1–6. https://doi.org/10.1109/pes.2011.6039527

Poole, D. L., & Mackworth, A. K. (2010). *Artificial Intelligence: Foundations of Computational Agents*.

Prehoda, E., Pearce, J., & Schelly, C. (2019). Policies to Overcome Barriers for Renewable Energy Distributed Generation: A Case Study of Utility Structure and Regulatory Regimes in Michigan. *Energies*, *12*(4), 674. https://doi.org/10.3390/en12040674

Qiu, D., Ye, Y., Papadaskalopoulos, D., & Strbac, G. (2021). Scalable coordinated management of peer-to-peer energy trading: A multi-cluster deep reinforcement learning approach. *Applied Energy*, *292*, 116940. https://doi.org/10.1016/j.apenergy.2021.116940

Robyns, B., Dobigny, L., Abbes, D., Durillon, B., Barry, H., & Saudemont, C. (2024). *Smart Grids and Buildings for Energy and Societal Transition*.

Sayigh, A. (2024). Solar and Wind Energy Will Supply More than 50% of World Electricity by 2030. *Transition Towards a Carbon Free Future*, 349–364. https://doi.org/10.1007/978-3-031-61660-0_22

Snell, T., & Bazen, A. (2024). Solar energy facts and. *American Journal of Applied Sciences*, *14*(3), 1–15.

Stephant, M. (2021). *Optimisation de l'autoconsommation dans une communauté énergétique locale via une blockchain*.

Stephant, M., Abbes, D., Hassam-Ouar, K., Labrunie, A., & Robyns, B. (2021). *Increasing photovoltaic self-consumption with game theory and blockchain*. *8* (34), 166770. https://doi.org/10.4108/eai.27-10-2020.166770

Swibki, T., Ben Salem, I., Kraiem, Y., Abbes, D., & El Amraoui, L. (2023). Imitation Learning-Based Energy Management Algorithm: Lille Catholic University Smart Grid Demonstrator Case Study. *Electronics*, *12*(24), 5048. https://doi.org/10.3390/electronics12245048

Tang, R., Wang, S., & Li, H. (2019). Game theory based interactive demand side management responding to dynamic pricing in price-based demand response of smart grids. *Applied Energy*, *250*, 118–130. https://doi.org/10.1016/j.apenergy.2019.04.177

United Nations. (2024). *Causes and effects of climate change*.

Wen, Q., Liu, G., Rao, Z., & Liao, S. (2020). Applications, evaluations and supportive strategies of distributed energy systems: A review. *Energy and Buildings*, *225*, 110314. https://doi.org/10.1016/j.enbuild.2020.110314

Yaddarabullah Akbar, Y. M., Rahman, A. B. A., & Saad, A. (2023). Measurement of Cooling Load-Based Occupant Behavior in Under-Actuated Zones: A Time-Variance Approach. *American Journal of Applied Sciences*, *20*(1), 48–64. https://doi.org/10.3844/ajassp.2023.48.64